Journal of Operation and Automation in Power Engineering
Vol. 5, No. 2, Dec. 2017, Pages: 215-225
http://journals.uma.ac.ir/joape

Dynamic Analysis and Optimal Design of FLPSS for Power Network Connected Solid Oxide Fuel Cell Using of PSO

*H. Shahsavari, A. Safari *, J. Salehi*

Department of Electrical Engineering, Azarbaijan Shahid Madani University, Tabriz, Iran.

Abstract- *This paper studies the theory and modeling manner of solid oxide fuel cell (SOFC) into power network and its effect on small signal stability. The paper demonstrates the fundamental module, mathematical analysis and small signal modeling of the SOFC connected to single machine infinite bus (SMIB) system. The basic contribution of the study is to attenuate the low frequency oscillations by optimal stabilizers in the presence of SOFC. To optimize the performance of system, fuzzy logic-based power system stabilizer (FLPSS) is exploited and designed by particle swarm optimization (PSO) technique. To ensure the effectiveness of the proposed optimal stabilizers, the simulation process takes in three scenarios of operating conditions. The effectiveness of proposed PSO based FLPSS on the oscillations in the power system, including SOFC is extensively demonstrated through time-domain simulations and by comparing FLPSS with the results of other stabilizers approaches.*

Keywords: Solid oxide fuel cell, Fuzzy logic-based PSS, Small signal model, Particle swarm optimization.

1. INTRODUCTION

Solid oxide fuel cell (SOFC) is a promising power generation technology, which produces electricity by oxidizing a fuel directly. The SOFCs are high temperature fuel cells, which demonstrate high potential to be used as clean power generation source in electrical network, because of numerous advantages such as fuel flexibility, inexpensive catalyst, solid electrolyte, availability of waste heat for combined heat and power (CHP) operation and high electrical efficiency. With the fast development of the SOFC technology, dynamic mathematical models become important topic. Demonstrative of the SOFC performance and structure have been presented in Refs. [1-3]. Authors in the Ref [2] discusses different fuel cell technologies, the various applications, and reviews their commercialization considerations and status. It is predictable that in the following many years, the SOFC with higher capacity will be regarded as source power generation in transmission network [4,5]. Therefore, the consequence of high capacity SOFC on small signal stability is important and must be investigated carefully [6-8]. Ref [6] describes the initial fuel cell stack and power conditioner modeling methodologies. Authors in the Ref [7,8] develops a comprehensive nonlinear dynamic model of a solid oxide fuel cell (SOFC) that can be used for dynamic and transient stability studies in two parts. One of the objectives of this paper is to gain a clear understanding of the effect of FC generation of system small-signal stability when it operates jointly with conventional power generation. So far, there have been many literatures in regards to the SOFC power plant on the stability of the distribution system. For example, Das and Co-workers in Ref. [9] represent the dynamic operation of the SOFC in the distribution system so that model works in island mode and in the grid connected mode. Eric et al. [10] present a model for the SOFC stack that operates at relatively low pressures and illustrate the dynamic behavior of the two models connected to the distribution system. Ref. [11] introduces dynamic models of micro-turbine and FC as dispersed generators and investigates its impact on the dynamic behavior of the system. Power system small-signal stability is generally affected by conventional generation, that is, the performance of synchronous generators. For last years, most studies of SOFC power plants have been on the operation grid-connected SOFC themselves, including development of mathematical model of SOFC power plants [12-13]. Authors in the literature [12] investigated the consequence of SOFC model integrated with the single machine infinite-bus (SMIB) system on the dynamic stability and show the size of the SOFC injected

Received: 29 Apr. 2017
Revised: 05 June 2017
Accepted: 01 July 2017
*Corresponding author:
E-mail: safari@azaruniv.ac.ir (A. Safari)
Digital object identifier: 10.22098/joape.2017.3563.1282

power generation to the grid consequences on damp torque. It will also help either positive or negative damping on low frequency oscillations, although not discussed about how exactly to control this system. Ref. [13] shows a reduced order dynamic model of gird-connected FC power generation that studies on the effect of the mixed between FC and gas-turbine generation on the dynamic stability. By forecasting the future of SOFC in interconnected power systems, it is important to study how the grid connection of SOFC generation can effectively and efficiently improve dynamic stability. The main motivation of this article is Heffron-Philips model of the SOFC power plant connected into large-scale power system and damp out the electromechanical oscillations by optimal stabilizer in an example case study. In particular, the un-damped power oscillations with frequency between 0.2 and 2.0 Hz, i.e., local and inter-area oscillations may jeopardize the system operation and cause the system instability [14-16]. In order to damp these power oscillations and increase stability, the power system stabilizer (PSS) installed to the synchronous generator has been successfully used in the presence of SOFC power plants. To optimize the performance of the system, the optimal stabilizer design is formulated as an optimization problem and the PSO is employed to solve this problem. The PSO is one of the most interesting heuristic algorithms which were first introduced by Kennedy and Eberhart. It can make a better solution within a shorter time than other random methods. So far, there have been many publications in the field of optimization with PSO, for example in Ref. [17], the problem of coordinated tuning of brushless exciter and classic power system stabilizer (PSS) parameters of a single machine is solved by PSO technique. The next phase, this paper provides an adjusted fuzzy logic-based PSS (FLPSS) parameters using particle swarm optimization algorithm. So far, there have been few publications about fuzzy logic-based PSO. Ref [18] presents a novel indirect adaptive power system stabilizer via a developed synergetic control methodology and fuzzy systems. Results evaluation reveals that the proposed controller achieves good and effective performance for damping of low frequency oscillations under different disturbances and is more advanced than the PSO based classic PSS.

The objectives of this study are:

- A comprehensive dynamic model of SOFC plants has been developed to study dynamic stability in power systems.
- The proposed model has a suitable complexity and integrity for attenuating the electromechanical oscillations.
- The PSO is employed to search for optimal classic PSS parameters, PID parameters and FLPSS parameters in the presence of SOFC connected to single-machine system.

The rest of the paper is organized as follows. In Section 2, detailed modeling of the power system components, including conventional units and high capacity SOFC, used for small signal stability studies, is introduced. Section 3 presents the optimal technique for designing different PSS for a power system incorporating SOFC. Additionally, the optimized parameters for PID, classic PSS and FLPSS are presented in this section. Section 4 shows and analyzes the time-domain results obtained from the proposed optimization model and solution approach. Finally, conclusions are summarized in Section 5.

2. PROBLEM MODEL

This research work studies the effects of a power system, including SOFC on the electro-mechanical oscillation modes of the power system. PSS design to increase the damping of these modes is also evaluated. For this purpose, different components of power system, including generators, their control systems and the SOFC power plant should be first modeled. Based on these outcomes, the system small signal stability can be evaluated. Then, by using the eigenvalues and deviation factors of the system, the optimal stabilizers are designed by PSO technique.

2.1. SOFC model

The SOFC produces DC electric power from fuel and oxidant via electrochemical process. The chemical reactions inside the cell that are directly involved in the production of electricity are given as [6-8]:

Anode: $$H_2 + O^{=} \rightarrow H_2O + 2e^{-} \quad (1)$$

Cathode: $$\frac{O_2}{2} + 2e^{-} \rightarrow O^{=} \quad (2)$$

The SOFC output power depends on its current. This means that the output power must control the output current. Therefore, we have:

$$I_{fc-ref} = \frac{P_{fc-ref}}{V_{fc}} \quad (3)$$

The SOFC should operate within the correct area, I_{fc-ref} is limited by the following boundaries:

$$I_{fc-ref\,\max} = \frac{U_{\max}}{2K_r} q_{h2-in} \quad (4)$$

$$I_{fc-ref\,\min}=\frac{U_{\min}}{2K_r}q_{h2-in}\qquad K_r=\frac{N_0}{4F} \tag{5}$$

where $U_{\max}$ and $U_{\min}$ is the maximum and minimum fuel unitization respectively. The N_0 is the number of cells in series in the FC stack, q_{h2-in} is the hydrogen input flow rate and F is the Faraday constant. Figure 1 shows the schematic of a SOFC connected to power network. The mathematical formulation of the SOFC is illustrated as follows [12]:

$$I_{fc}=\frac{1}{1+T_e s}I_{fc-ref} \tag{6}$$

$$q_{h2-in}=\frac{2K_r}{U_{opt}}\frac{1}{1+T_f s}I_{fc-ref} \tag{7}$$

$$q_{o2-in}=\frac{1}{r_{ho}}q_{h2-in} \tag{8}$$

$$p_{h2}=\frac{1}{K_{h2}}\frac{1}{1+T_{h2}s}\left(q_{h2-in}-2K_r I_{fc}\right) \tag{9}$$

$$p_{o2}=\frac{1}{K_{o2}}\frac{1}{1+T_{o2}s}\left(q_{o2-in}-K_r I_{fc}\right) \tag{10}$$

$$p_{h2o}=\frac{1}{K_{h2o}}\frac{1}{1+T_{h2o}s}2K_r I_{fc} \tag{11}$$

U_{opt} is the optimal fuel utilization, T_f is the time constant of dynamic of fuel supply, r_{ho} is the ratio of hydrogen to oxygen, K_{h2}, K_{o2} and K_{h2o} is the valve molar constant for hydrogen, oxygen and water, T_{h2}, T_{o2} and T_{h2o} is the time constant for hydrogen, oxygen and water flow respectively. By using of the Nernst relation, the internal Emf generated by the FC stack can be formulated as:

$$V_{fc}=N_0\left[E_0+\frac{RT}{2F}\ln\left(\frac{p_{h2}\times p_{o2}^{0.5}}{p_{h2o}}\right)\right]-rI_{fc} \tag{12}$$

where E_0 is the voltage associated with the reaction-free energy of a cell, R is the gas constant, T is the SOFC operating temperature typically in the range of 800° C–1000° C, p_{h2}, p_{o2}, and p_{h2o} are the reactant partial pressures of hydrogen, oxygen and water, respectively.

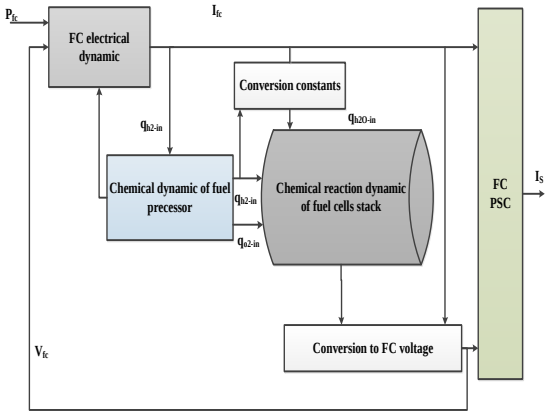

Fig. 1. Schematic of the SOFC

2.2. Synchronous generator model

Mathematical model of the synchronous generator can be as follows [19]. In $d-q$ coordinate of the generator, I_{ts} was shown by its d and q component i_{tsd} and i_{qsd} respectively.

$$\dot{\sigma}=\omega_0(\omega-1) \tag{13}$$

$$\dot{\omega}=\frac{1}{M}\left(P_m-P_t-D(\omega-1)\right) \tag{14}$$

$$\dot{E}_q^{'}=\frac{1}{T_{d0}^{'}}\left(E_{fd}-E_q^{'}+\left(x_d-x_d^{'}\right)i_{tsd}\right) \tag{15}$$

$$\dot{E}_{fd}=-\frac{1}{TA}E_{fd}^{'}+\frac{KA}{TA}\left(V_{ref}-V_t\right) \tag{16}$$

Where

$$P_t=E_q^{'}i_{tsq}+(x_q-x_d^{'})i_{tsd}i_{tsq} \tag{17}$$

$$V_t=\sqrt{(x_q i_{tsq})^2+(E_q^{'}-x_d^{'}i_{tsd})^2} \tag{18}$$

2.3. Modeling of SOFC in SMIB

Figure 2 illustrates the configuration of the SOFC power generation connected to the SMIB system. x_s, x_{sb1}, x_{sb2} and x_{ts} denote the equivalent reactance of transformers or/and transmission line. Parameters of a case study are given in Appendix. Since the level of SOFC output voltage for connecting to the power network is low, as result the dc-dc boost converter is exploited. The control of SOFC output current is realized with a dc-dc converter. Hence, we have:

$$d=d_0+T_d\left(I_{fc-ref}-I_{fc}\right) \tag{19}$$

where d is the duty cycle and T_d the transfer function of the FC current controller.

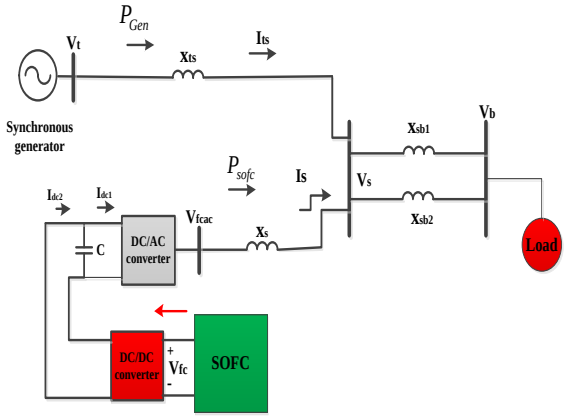

Fig. 2. Configuration of the SOFC power generation connected to SMIB system

Operating in continuous conduction mode (CCM) is shown in Figure 3 by using of the state space averaging method to a dc-dc boost converter. The boost converter has two different linear circuits [20]. First, the switch is on, second, the switch is off.

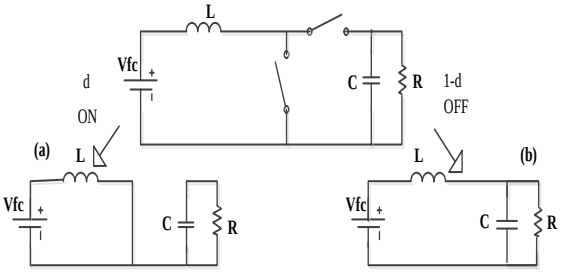

Fig. 3. Operating of DC-DC converter in two stages of switching

State space models for Fig. 3(a) and (b) can be formulated as follows, respectively:

$$\begin{aligned} \dot{x} &= A_{on}x + B_{on}u \\ y &= C_{on}x + D_{on}u \end{aligned} \tag{20}$$

$$\begin{aligned} \dot{x} &= A_{off}x + B_{off}u \\ y &= C_{off}x + D_{off}u \end{aligned} \tag{21}$$

These can be approximated by the following state space averaged model.

$$\begin{aligned} \dot{X} &= AX + Bu \\ Y &= CX + Du \end{aligned} \tag{22}$$

$$\begin{aligned} A &= dA_{on} + (1-d)A_{off} \qquad C = dC_{on} + (1-d)C_{off} \\ B &= dB_{on} + (1-d)B_{off} \qquad D = DA_{on} + (1-d)D_{off} \end{aligned} \tag{23}$$

Therefore,

$$\dot{i}_L = \frac{V_c \times d}{L} - \frac{V_C}{L} + \frac{V_{fc}}{L} \tag{24}$$

$$\dot{V}_C = \frac{i_L}{C} - \frac{d \times i_L}{C} - \frac{V_C}{RC} \tag{25}$$

where $\dot{i}_L$ is the DC-DC inductor current and V_c is the DC-DC capacitor voltage.

After changing the DC voltage level, a dc-ac converter will be needed for connecting to the power system. The ac voltage at the terminal of the converter can be calculated as follows [21]:

$$\bar{V}_{fcac} = mkV_{dc}\left(\cos\psi + j\sin\psi\right) \tag{26}$$

where V_{dc} is the terminal voltage of DC-DC converter, ψ is the angle deviation between V_{fcac} and V_{dc} and k is usually equal to 0.75 [21].

The dc-ac converter has two different controllers. m is the modulation ratio and φ is the phase of the pulse width modulation (PWM).

$$\phi = \phi_0 + T_{vdc}(s)\left(V_{dc} - V_{dc-ref}\right) \tag{27}$$

$$m = m_0 + T_{vac}(s)\left(V_s - V_{s-ref}\right) \tag{28}$$

where T_{vdc} is transfer function of the DC voltage controller and T_{vac} is transfer function AC voltage controller.

From Fig. 2, mathematical formulation of the dc-ac converter can be stated as:

$$\dot{V}_{dc} = \frac{1}{C_{dc}}\left(I_{dc2} - I_{dc1}\right) \tag{29}$$

We can have:

$$\bar{V}_t = jx_{ts}\bar{I}_{ts} + \bar{V}_s \tag{30}$$

$$\bar{V}_s = -j(x_s)\bar{I}_s + \bar{V}_{fcac} \tag{31}$$

$$\bar{V}_s - \bar{V}_b = jx_{sb}\left(\bar{I}_{ts} + \bar{I}_s\right) \quad x_{sb} = x_{sb1} \parallel x_{sb2} \tag{32}$$

The relations are transferred to d-q frame of the synchronous machine. Hence, we have:

$$\begin{bmatrix} x_{sb} & x_s + x_{sb} \\ x_q + x_{ts} + x_{sb} & x_{sb} \end{bmatrix}\begin{bmatrix} i_{tsq} \\ i_{sq} \end{bmatrix} = \begin{bmatrix} -V_{fcac}\cos\psi + V_b\sin\delta \\ V_b\sin\delta \end{bmatrix} \tag{33}$$

$$\begin{bmatrix} x_{sb} & x_s + x_{sb} \\ x_d' + x_{ts} + x_{sb} & x_{sb} \end{bmatrix}\begin{bmatrix} i_{tsd} \\ i_{sd} \end{bmatrix} = \begin{bmatrix} V_{fcac}\sin\psi - V_b\cos\delta \\ E_q' - V_b\cos\delta \end{bmatrix} \tag{34}$$

2.4. Linearized Model

Linearization of a dynamic model of the dc-dc converter Eqs. (24) and (25) can be obtained the following:

$$\Delta \dot{i}_{fc} = \frac{V_{fcac0}}{L}\Delta d + \frac{(d_0 - 1)}{L}\Delta V_c + \frac{1}{L}\Delta V_{fc} \quad (35)$$

$$\Delta \dot{V}_c = -\frac{i_{fc0}}{C}\Delta d + \frac{(1-d_0)}{C}\Delta V_c - \frac{1}{RC}\Delta V_{fc} \quad (36)$$

$$\Delta \dot{d} = -T_1 \Delta \dot{i}_{fc} - T_2 \Delta i_{fc} \quad (37)$$

For dc-ac converter, we have:

$$\Delta \dot{V}_{dc} = \frac{1}{C_{dc}}(\Delta I_{dc2} - \Delta I_{dc1}) \quad (38)$$

$$\Delta\phi = T_{vdc}(s)\Delta V_{dc} \quad (39)$$

$$\Delta m = -T_{vac}(s)\Delta V_s \quad (40)$$

Linearized of Eqs. (33) and (34) is denoted by the following:

$$\begin{bmatrix}\Delta i_{tsd} & \Delta i_{tsq}\end{bmatrix}^T = Q\begin{bmatrix}\Delta\delta & \Delta E_q^{'} & \Delta V_{dc} & \Delta m & \Delta\psi\end{bmatrix}^T \quad (41)$$

$$\begin{bmatrix}\Delta i_{sd} & \Delta i_{sq}\end{bmatrix}^T = W\begin{bmatrix}\Delta\delta & \Delta E_q^{'} & \Delta V_{dc} & \Delta m & \Delta\psi\end{bmatrix}^T \quad (42)$$

Where,

$$Q = \begin{bmatrix} Q_{11} & Q_{12} & Q_{13} & Q_{14} & Q_{15} \\ Q_{21} & Q_{22} & Q_{23} & Q_{24} & Q_{25} \end{bmatrix}$$
$$W = \begin{bmatrix} W_{11} & W_{12} & W_{13} & W_{14} & W_{15} \\ W_{21} & W_{22} & W_{23} & W_{24} & W_{25} \end{bmatrix} \quad (43)$$

Linearization of the SOFC power generation can be written as:

$$\Delta I_{fc-ref} = -\frac{P_{fc-ref}}{V_{fc0}^2}\Delta V_{fc} \quad (44)$$

$$\Delta I_{fc} = \frac{1}{1+T_e s}\Delta I_{fc-ref} \quad (45)$$

$$\Delta q_{o2-in} = \frac{1}{r_{ho}}\Delta q_{h2-in} \quad (46)$$

$$\Delta q_{h2-in} = \frac{2K_r}{U_{opt}}\frac{1}{1+T_f s}\Delta I_{fc-ref} \quad (47)$$

$$\Delta p_{h2} = \frac{1}{K_{h2}}\frac{1}{1+T_{h2}s}\left(\Delta q_{h2-in} - 2K_r\Delta I_{fc}\right) \quad (48)$$

$$\Delta p_{o2} = \frac{1}{K_{o2}}\frac{1}{1+T_{o2}s}\left(\Delta q_{o2-in} - K_r\Delta I_{fc}\right) \quad (49)$$

$$\Delta p_{h2o} = \frac{1}{K_{h2o}}\frac{1}{1+T_{h2o}s}2K_r\Delta I_{fc} \quad (50)$$

$$\Delta V_{fc} = a_1\Delta p_{h2} + a_2\Delta p_{o2} + a_3\Delta p_{h2o} + a_4\Delta I_{fc} \quad (51)$$

By using of Eqs. (33) and (34), linearized of Eqs. (17) and (18) is denoted by the following:

$$\Delta P_t = K_1\Delta\delta + K_2\Delta E_q^{'} + K_{pdc}\Delta V_{dc} + \ldots K_{pm}\Delta m + K_{p\psi}\Delta\Psi \quad (52)$$

$$\Delta E_q = K_4\Delta\delta + K_3\Delta E_q^{'} + K_{qdc}\Delta V_{dc} + \ldots K_{qm}\Delta m + K_{q\psi}\Delta\Psi \quad (53)$$

$$\Delta V_t = K_5\Delta\delta + K_6\Delta E_q^{'} + K_{vdc}\Delta V_{dc} + \ldots K_{vm}\Delta m + K_{v\psi}\Delta\Psi \quad (54)$$

Thus, linearization of the generator shown by Eqs. (13) - (16) can be calculated the following:

$$\Delta\dot{\sigma} = \omega_0\Delta\omega \quad (55)$$

$$\Delta\dot{\omega} = \frac{1}{M}\left(-K_1\Delta\delta - D\Delta\omega - K_2\Delta E_q^{'} - \ldots K_{pdc}\Delta V_{dc} - K_{pm}\Delta m - K_{p\psi}\Delta\psi\right) \quad (56)$$

$$\Delta\dot{E}_q^{'} = \frac{1}{T_{d0}^{'}}\left(-K_4\Delta\delta - K_3\Delta E_q^{'} - K_{qdc}\Delta V_{dc} - \ldots K_{qm}\Delta m - K_{q\psi}\Delta\psi + \Delta E_{fd}^{'}\right) \quad (57)$$

$$\Delta\dot{E}_{fd}^{'} = -\frac{1}{T_A}\Delta E_{fd}^{'} - \frac{KA}{T_{d0}^{'}}\left(K_5\Delta\delta + K_6\Delta E_q^{'} + K_{vdc}\Delta V_{dc} + \ldots K_{vm}\Delta m + K_{v\psi}\Delta\psi\right) \quad (58)$$

By using of the obtained Eqs. (39), (40), (44), (45), (46), (47), (48), (49), (50), (55), (56), (57) and (58), the block diagram of the system can be shown (Fig. 4). In the next section, controller design for the sample test case is reviewed.

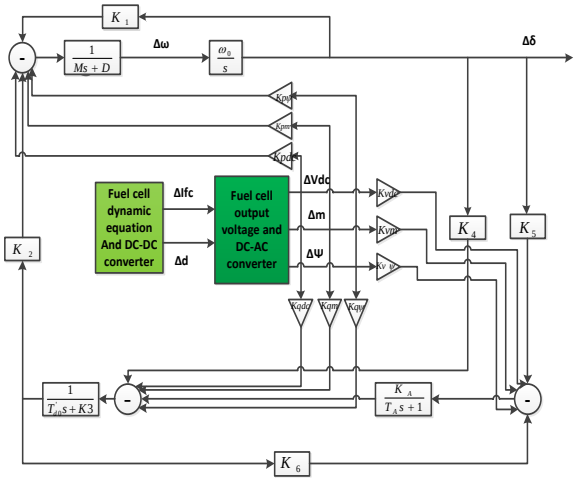

Fig. 4. Linearized model of the SOFC in SMIB

3. SOLUTION METHODOLOGY

3.1. Particle swarm optimization

The PSO has been just a population based stochastic optimization technique developed by Eberhart and Kennedy [22], motivated by social behavior of bird flocking or fish schooling. Generally, the PSO is characterized as a straightforward concept, computationally efficient and easy to implement [23-25]. The features of the strategy are it based on a simple concept and developer for nonlinear optimization problems with continuous variables. The PSO is spread through simulation in two-dimension space. The positioning of every agent is shown by XY axis position. Each agent knows its best value so far (*pbest*) and its position also knows the most effective value so far in the group (*gbest*). Each agent tries to modify its position utilizing the following:

$$v_i^{k+1} = wv_i^k + c_1 rand_1 \times (pbest_i - s_i^k) + ... \\ c_2 rand_2 \times (gbest - s_i^k) \quad (59)$$

$$s_i^{k+1} = s_i^k + v_i^{k+1} \quad (60)$$

where v_i^{k+1} is the velocity of agent *i*th at iteration *k*th, w is weighting function, c_i is weighting factor, $rand$ is random number between 0 and 1, s_i^k is the current position of the agent *i*th at iteration *k*th and s_i^{k+1} is modified searching point. The weighting function is given by:

$$w = -\frac{w_{\max} - w_{\min}}{iter_{\max}} \times iter \quad (61)$$

Where $w_{\max}$ is initial weight , $w_{\min}$ is final weight , $iter_{\max}$ is a maximum iteration number, $iter$ is current iteration. The details of the illustration and the flowchart of PSO are given in [22].

3.2. Fuzzy logic method

Fuzzy logic based-power system stabilizer (FLPSS) is exploited and designed by PSO technique to damp the oscillation as a result of imported disturbance. The input of the FLPSS may be the speed deviation ($\Delta\omega$) and power deviation (Δp) and also the output is injected into the excitation system. The target of this controller is to improve the damping of the oscillation due to disturbance of the system. The power deviation (Δp), speed deviation ($\Delta\omega$) and the fuzzy output signal (O) are divided into seven triangular shape membership functions with range [-0.8 , 0.8]. Fig.5 shows the related membership functions [17]. The membership functions are described by [Negative Big (NB), Negative Medium (NM), Negative small (NS), Zero (ZE), Positive Small (PS), Positive Medium (PM), Positive Big (PB)]. An output signal (O) is described by [Output Negative Big (ONB), Output Negative Medium (ONM), output Negative Small (ONS), Output Zero (OZE), Output Positive Small (OPS), Output Positive Medium (OPM), Output Positive Big (OPB)]. The fuzzy control rules designed by previous experience of the controlled dynamic system are shown in Table 1.

3.3. Optimal design of stabilizers for SOFC in SMIB

3.3.1. Optimal tune of inverter PID controller

In this section, two control signals, Δm and $\Delta\varphi$ are reviewed. The controller structure considered for these signals is PID controller, which is shown in Fig. 6. The PSS is not installed to synchronous generator. The parameters of PID controller $KI_{1,2}$ $KD_{1,2}$ $KP_{1,2}$ should be tuned by PSO algorithm. The eigenvalue based objective function is denoted by the following:

$$OF = Min\ [Max\ (\lambda_i) + \sum_{j=1}^{n} (1 - \xi_j)]\quad i = 1,2,...n, \quad (62)$$

where λ is the real of eigenvalues, n is the total number of the eigenvalues and ξ_j is the damping ratio. The objective of the optimization problem is to maximize the damped oscillation due to imported disturbance. According to the simulation, the following PSO parameters are used for searching for the controllers parameters:

- Iteration=100
- Population size = 50
- Inertia weight factor w is set by Eq. (61) here w_{max} = 0.9 and w_{min} = 0.4.
- Acceleration constant c_1 = 2 and c_2 = 2.

The best solution that obtained is summarized in Table 2.

3.3.2 Optimal tuning of classic PSS

The classic power system stabilizers shown in Fig. 7. The details of the block diagram can be found in [14]. In this section, the parameters of exciter T_A, K_A and PSS $T_1 - T_4$ and K_C should be tuned with the PSO in a case study. The input and output of the PSS is the speed deviation $\Delta\omega$ and the excitation voltage, respectively. The objective function in this section is exactly the same as the objective function in the previous section. The lower and upper limits of the PSS and exciter parameters are given in Table 3. The best solution obtained is given in Table 4.

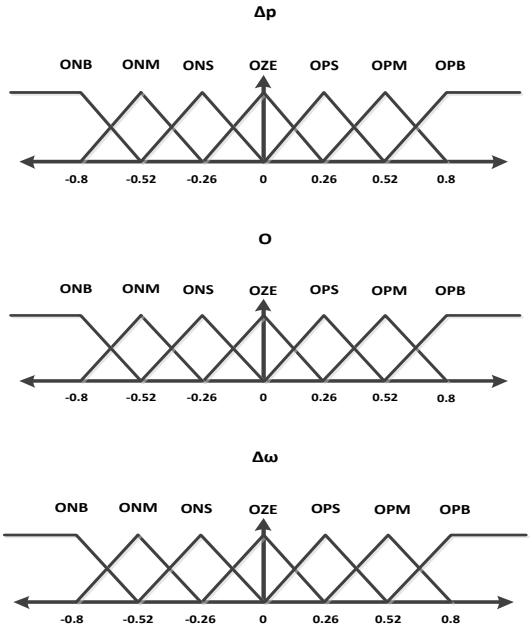

Fig. 5. Membership function of fuzzy logic based controller

Table 1. Rules for the FLPSS

Speed deviation ($\Delta\omega$)	Power deviation (Δp)						
	NB	NM	NS	ZE	PS	PM	PB
NB	ONB	ONB	ONB	ONB	ONS	ONS	OZE
NM	ONB	ONB	ONM	ONM	ONS	OZE	OPS
NS	ONB	ONM	ONM	ONS	OZE	OPS	OPM
ZE	ONM	ONM	ONS	OZE	OPS	OPM	OPM
PS	ONM	ONS	OZE	OPS	OPM	OPM	OPB
PM	ONS	OZE	OPS	OPM	OPM	OPB	OPB
PB	OZE	OPS	OPM	OPB	OPM	OPB	OPB

Table 2. Optimal values of PID controller

Parameters	KI_1	KD_1	KP_1	KI_2	KD_2	KP_2
Optimal value	5.6e-7	1.0	-1.1	2.7	0	0.36

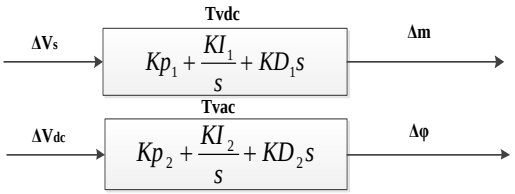

Fig. 6. PID controller for the inverter

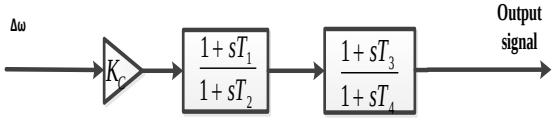

Fig. 7. The power system stabilizer

Table 3. Lower and upper limits of PSS and exciter parameters

Parameters	Lower band	Upper band
T_1	1	3
T_2	0.01	0.3
T_3	1	3
T_4	0.01	3
K_C	1	5
TA	0.05	0.9
KA	5	20

Table 4. Optimal values of PSS and exciter parameters

Parameters	Optimal value
T_1	2.5
T_2	0.06
T_3	1.09
T_4	0.17
K_C	2.5
TA	0.14
KA	6.5

3.3.3 Optimal tuning of FLPSS

The choice of suitable parameter for the fuzzy logic method plays an essential role in achieving the controller goals. Since the FLPSS has two inputs and one output, it has $K\omega$ andKP parameters for input and KO parameter for output signal. These parameters are tuned with PSO. The system equipped with FLPSS is shown in Fig. 8. The computational flow chart of PSO based FLPSS is shown in Fig. 9. The objective function to tuning of FLPSS is defined by the following:

$$OF = Min(\sum abs(\Delta\omega) + OS + j),$$
$$OS = \frac{r-y}{} \times 100, \quad (63)$$
$$j = \sum^{r} te^2,$$

Where OS is the system overshoot, j is the performance index, e is the system error, t is the time, r is the system reference, and y is the system output. The goal of this objective function is to improve the damping of the oscillation and reducing the system overshoot and settling time.

The lower band and upper band limits of the three parameters are given in Table 5. The optimal parameters are shown in Table 6.

4. Simulation Results

To evaluate the small signal modeling of the SOFC connected to SMIB system and proposed stabilizers,

three scenarios will be considered (Table 7).

4.1 Scenario 1

The simulation of the system is tested by a mechanical torque entered into the generator. Figure 10 shows the speed deviation of a single machine system without a controller. Under this condition, it can be seen that the system is stable after highly oscillations.

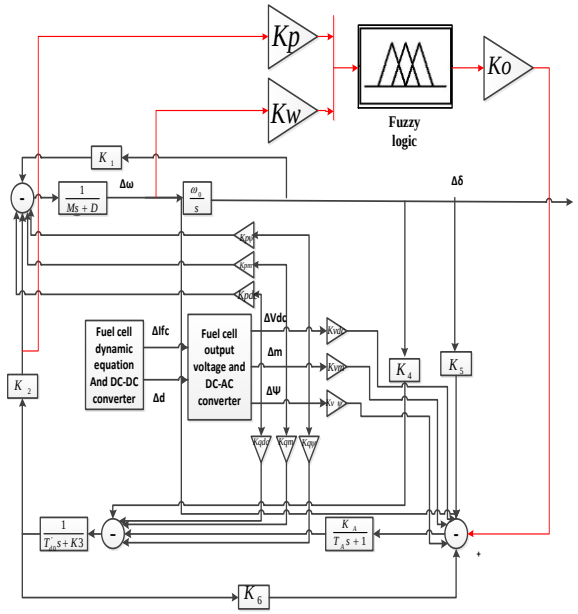

Fig. 8. The system equipped with FLPSS

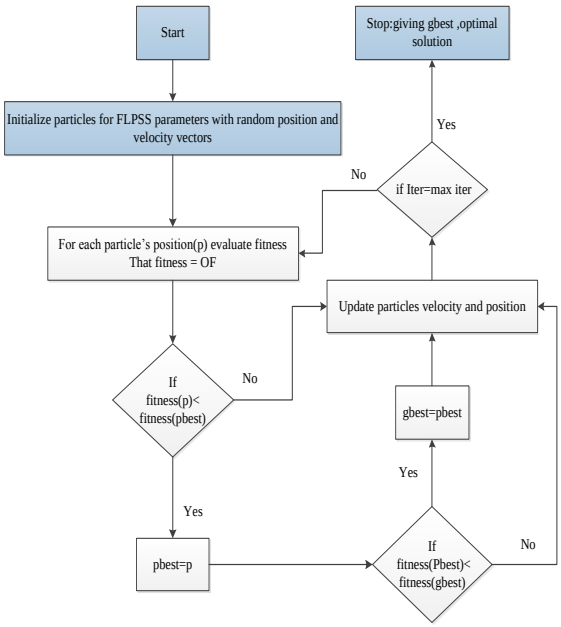

Fig. 9. A flowchart of PSO based FLPSS

Table 5. Lower and upper limits of FLPSS parameters

Parameters	$K\omega$	KP	KO
Lower band	4	0.1	0.1
Upper band	30	3	1.5

Table 6. The optimal values of Fuzzy logic based power system stabilizer parameters

Parameters	$K\omega$	KP	KO
Optimal value	15.02	1.06	0.7

Table 7. Considered scenarios

Senario 1	$P_{SOFC} = 0.3$	$P_{Gen} = 0.7$
Senario 2	$P_{SOFC} = 0.7$	$P_{Gen} = 0.3$
Senario 3	$P_{SOFC} = 0.9$	$P_{Gen} = 0.1$

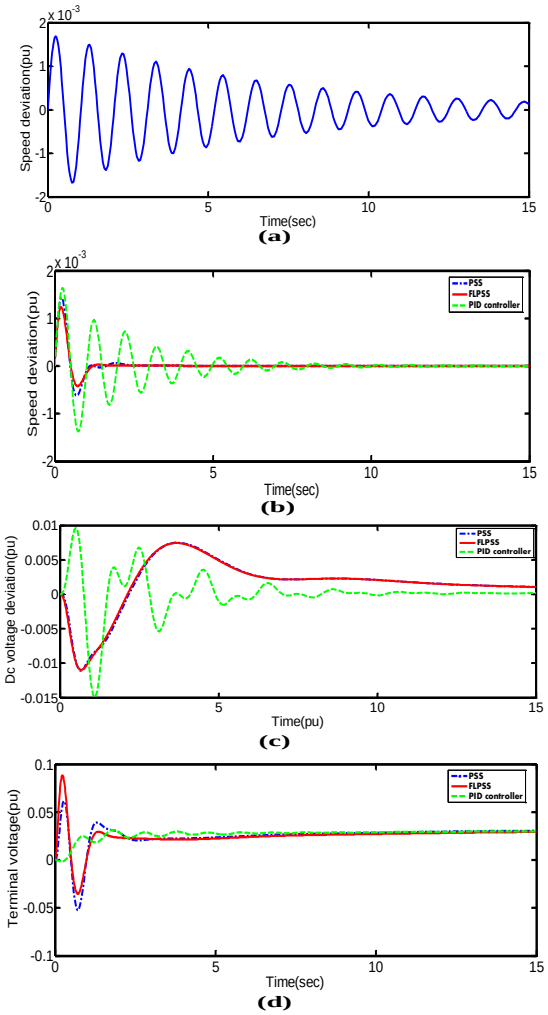

Fig. 10.Outputsignals of SOFC connected to SMIB system in scenario 1

Figure 10 (a) shows the plot of speed deviation response of the equipped generator with different stabilizers under the electromechanical disturbance. By visual inspection of the curves in Fig. 10 (b), it can be seen that the speed deviation of the system equipped with FLPSS reached a better damping against another stabilizers. Although the speed deviation with tuned PID controller and PSO based classic PSS reached a relatively good damping. It is noticed that the speed deviation with PSO based FLPSS is better than that with PSO based

classic PSS with less settling time and overshoot.

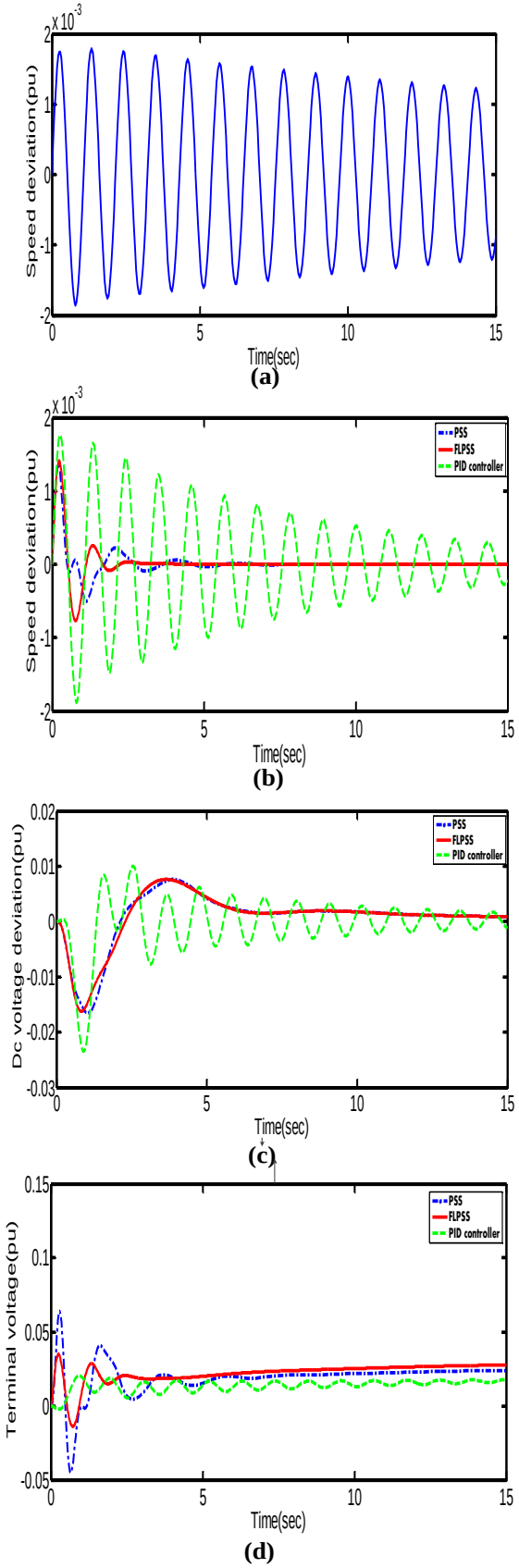

Fig. 11. Outputsignals of SOFC connected to SMIB system in scenario 2

Figure 10 (c) shows the DC voltage deviation of output DC-DC converter with different controllers. The DC voltage deviation with regulated classic PSS and regulated FLPSS is nearly the same. In this case the PID controller is better settling time than the others, but FLPSS has less overshoot. The terminal voltage deviation of single machine with different controller is shown in Fig. 10 (d), which demonstrates that the FLPSS has a better response.

4.2. Scenario 2

In this scenario, the SOFC power generation injected into the grid is more than the previous scenario. The speed deviation of a single machine system without controller shown in Fig.11 (a) demonstrates that the system reached to stability slower than when the SOFC power generation injected into the grid is less. Therefore, the size of the SOFC power generation injected into the grid can collaborate either positive or negative damping to low frequency oscillations. The speed deviation of the system with different controllers in this scenario is shown in Fig.11 (b). In this case, also the PSO based FLPSS reached a better damping than the other controllers. The dc voltage deviation of output dc-dc converter with different controllers is shown in Fig.11 (c). Also the terminal voltage deviation of single machine with different controller is shown in Fig.11 (d) that the FLPSS has a less overshoot and slower settling time.

4.3. Scenario 3

In this case, the SOFC power generation injected into the grid is more than previous scenarios. The speed deviation of a single machine system without controller is shown in Fig.12 (a) that the system is unstable after high oscillations. Therefore, the SOFC power generation can makes instability in the system. The speed deviation of the system with different controllers is shown in Fig 12 (b). As shown, the FLPSS and classic PSS can stable the system. The speed deviation with PSO based FLPSS is better than that with PSO based classic PSS with less settling time and overshoot. Also the dc voltage deviation of output dc-dc converter and terminal voltage deviation of single machine with different controllers are shown in Fig. 12 (c) and Fig. 12 (d) respectively.

5. Conclusions

This paper presents the consequence of the grid-connected SOFC power generation on small signal stability in power system and optimal design of the stabilizers to attenuate the low frequency oscillations. It is concluded that when the penetration of SOFC generation is more, the system reached to stability slower as well as becomes unstable. Therefore, the size of the

SOFC power generation injected into the grid can help either positive or negative damping to low frequency oscillations.

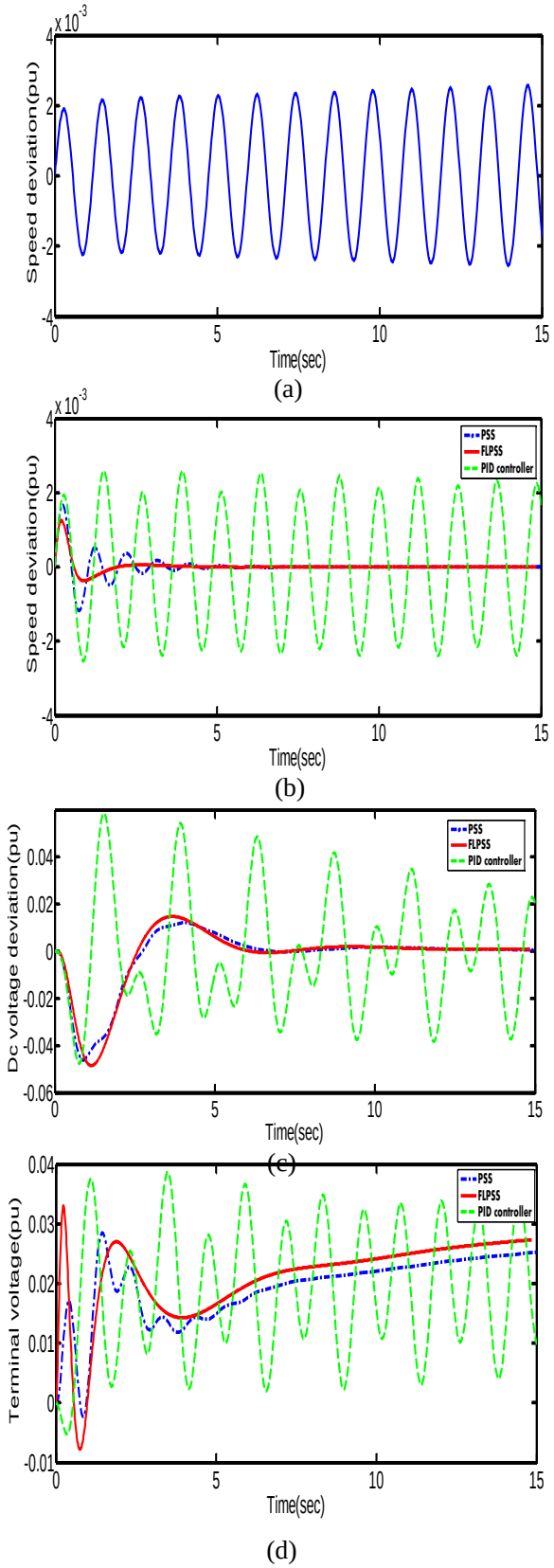

Fig. 12. Outputsignals of SOFC connected to SMIB system in scenario 3

A fuzzy logic-based control design is proposed for attenuate the low frequency oscillations of imported disturbance in power system in presence of a SOFC power generation. The optimization of parameters the FLPSS, classic PSS and PID controller is carried out. To acquire the optimized parameters, the PSO algorithm is applied to solve the design problem. Simulation study in the SMIB connected to the SOFC power generation confirms that the stabilizing consequence of the proposed PSO based FLPSS are much superior to those of the conventional classic PSS and PID controller.

APPENDIX

Data for the single machine infinite bus is [14]:

Transmission line			
$x_{ts} = 0.3\ p.u.$	$x_{sb1} = 0.4\ p.u.$	$x_{sb2} = 0.4\ p.u.$	$x_s = 0.3\ p.u.$

Generator	
x_d	1.3 p.u.
x_q	0.47 p.u.
x'_d	0.3 p.u.
M	7.4 s
D	4 p.u.
T'_{d0}	5 s

AVR	
$T_A = 0.1\ s$	$K_A = 10\ p.u.$

Initial condition	
V_{t0}	1.0 p.u.
V_{s0}	1.0 p.u.
V_{b0}	1.0 p.u.
V_{dc0}	1.0 p.u.

Parameters of the SOFC	
$T = 1273^{\circ}K.$	$F = 96487$
$R = 8.314$	$E_0 = 1.18V$
$N_0 = 384$	$K_r = 0.966e-6\ mol/(s.A)$
$U_{\max} = 0.9$	$U_{\min} = 0.8$
$U_{opt} = 0.85$	$t_{o2} = 2.91s$
$t_{h2} = 26.1s$	$K_{h2} = 5.43e-4\,mol/(s.atm)$
$t_{h2o} = 78.3s$	$K_{o2} = 2.52e-3\ mol/(s.atm)$
$r = 0.126\,\Omega$	$K_{h2o} = 2.81e-4\,mol/(s.atm)$
$T_f = 5s$	$T_e = 0.08s$
$r_{ho} = 0.8$	

REFERENCES

[1] J. Larminie and A. Dicks., *Fuel Cell System Explained*, 2nd. New York, Wiley, 2002.

[2] M. Farooque and H. C. Maru., "Fuel cells-the clean and

efficient power generators," *Proc. IEEE*, vol. 89, no.12, pp. 1819-1829, 2001.

[3] B. Raton, *Fuel Cell Technology Handbook*., FL: CRC, 2002.

[4] P. Thounthong, B. Davat, S. Rael, P. Sethakul., "Fuel cell high-power applications," *IEEE Ind. Electron. Mag.,* vol. 3, no. 1: pp. 32-46, 2009.

[5] Y. H. Li, S. Rajakaruna and S. S. Choi., "Control of a solid oxide fuel cell power plant in a grid-connected system," *IEEE Trans. Energy Coners.,* vol. 22, no. 2, pp. 405-413, 2007.

[6] J. Padulle's, G. W. Ault, and J. R. McDonald., "An integrated SOFC plant dynamic model for power systems simulation," *J. Power Sources*, vol. 86, pp. 495-500, 2000.

[7] K. Sedghisigarchi and A. Feliachi., "Dynamic and transient analysis of power distribution systems with fuel cells–part I: fuel-cell dynamic model," *IEEE Trans. Energy Convers.,* vol. 19, no. 2, pp. 423-428, 2004.

[8] K. Sedghisigarchi and A. Feliachi., "Dynamic and transient analysis of power distribution systems with fuel cells–part II: control and stability enhancement," *IEEE Trans. Energy Convers.*, vol. 19, no. 2, pp. 429-434, 2004.

[9] S. Das, D. Das and A. Patra., "Operation of solid oxide fuel cell based distributed generation," *Energy Procedia*, vol. 31; pp. 439-447, 2009.

[10] E. M. Fleming and I. A. Hiskens., "Dynamics of a microgrid supplied by solid oxide fuel cells in bulk power system dynamics and control-VII." *IEEE Revitalizing Oper. Reliab.,* vol. 19, pp. 1-10, 2007.

[11] H. Wang and G. Li., "Dynamic performance of microturbine and fuel cell in a microgrid," *Proc. Int. Conf. Mechatron. Sci. Electr. Eng. Comput.,* pp. 122-125, 2011.

[12] W. Du, H. F. Wang, X.F. Zhang and L.Y. Xiao., "Effect of grid-connected solid oxide fuel cell power generation on power systems small-signal stability," *IET Renew. Power Gener.*, vol. 6, no.1, pp. 24-37, 2012.

[13] C. J. Hatziadoniu, A. A. Lobo, F. Pourboghrat and M. Daneshdoost., "A simplified dynamic model of grid-connected fuel-cell generators," *IEEE Trans. Power Delivery,* vol. 17, no. 2, pp. 467-473, 2002.

[14] P. Kunder, *Power system stability and control*, McGraw-Hill, 1994.

[15] X. Yang and A. Feliachi., "Stabilization of inter-area oscillation modes through excitation systems," *IEEE Trans. Power Syst.*, vol. 9, no.1, pp.494-502, 1994.

[16] M. Klein, G. J. Roger and P. Kundur., "A fundamental study of inter-area oscillations in power systems," *IEEE Trans. Power Syst.,* vol. 6, no. 3, pp. 914-921, 1991.

[17] A. M. El-Zonkoly, A. A. Khalil and N. M. Ahmied., "Optimal tuning of lead-lag and fuzzy logic power system stabilizers using particle swarm optimization," *Expert Syst. Appl.* ,vol. 36, no. 2, pp. 2097-2106, 2009.

[18] K. Mazlumi, M. Darabian and M. Azari., "Adaptive fuzzy synergetic PSS design to damp power system oscillations," *J. Oper. Autom. Power Eng.*, vol. 1, no. 1, pp. 43-53, 2013.

[19] Y. N. Yu, *Electric power system dynamics*, Academic Press, Inc., 111 FIFTH AVE., NEW YORK, NY 10003, USA, 1983.

[20] M. R. Banaei., "Multi-Stage DC-AC Converter Based on new DC-DC converter for energy conversion," *J. Oper. Autom. Power Eng.*, vol. 4, no. 1, pp. 42-53, 2016.

[21] CIGRE technical report: Modeling of power electronics equipment (FACTS) in load flow and stability programs, CIGRE T F 38-01-08, 1998.

[22] J. Kennedy and R. Eberhart., "Particle swarm optimization," *Proc. IEEE Int. Conf. Neural Networks*, vol. 4, pp. 1942-1948, 1995.

[23] A. Jalilvand, A. Safari and R. Aghmasheh, "Design of state feedback stabilizer for multi-machine power system using PSO algorithm," *Proc. IEEE Int. Conf. Multitopic,* 2008, pp. 1-6.

[24] M. Rahmati, R. Effatnejad and A. Safari, "Comprehensive learning particle swarm optimization for multi-objective optimal power flow," *Indian J. Sci. Technol.,* vol. 7, no. 3, pp. 262-270, 2014.

[25] A. Safari, N. Rezaei, "Towards an extended power system stability: An optimized GCSC-based inter-area damping controller proposal," *Int. J. Electr. Power Energy Syst.*, vol. 56, pp. 316-324, 2014.